ELSEVIER

Journal of Nuclear Materials 275 (1999) 194–200

journal of nuclear materials

www.elsevier.nl/locate/jnucmat

Synergistic interaction of fatigue and stress corrosion on the corrosion fatigue crack growth behavior in Alloy 600 in high temperature and high pressure water

W.Y. Maeng [a,*], Y.H. Kang [a], T.W. Nam [b], S. Ohashi [c], T. Ishihara [d]

[a] *Korea Atomic Energy Research Institute, P.O. Box 105, Yusong, Taejon, South Korea*
[b] *Hanyang University, Taehak-dong 396, Ansan, South Korea*
[c] *National Research Istitute for Metal, 1-2-1, Senger, Tsukuba-shi, Ibaraki 305, Japan*
[d] *Yokohama National University, 156 Tokiwadei, Hodogaya-ku, Yokohama 240, Japan*

Received 2 October 1998; accepted 5 April 1999

Abstract

Three different types of cracking loads which simulate fatigue, stress corrosion cracking (SCC) and the combined fracture process of fatigue and SCC were applied to compact tension type Alloy 600 specimens in high temperature water at 290°C with 4 ppm dissolved oxygen concentration in order to evaluate the effects of various load applications on corrosion fatigue crack growth in Alloy 600. The measured crack growth rate of the specimen to which combined loads of fatigue and SCC were applied was faster than the predicted crack growth rate based on the superposition model. The increase in the crack growth rate indicates that there is a synergistic interaction of fracture processes at the growing crack tip which experiences combined loads of SCC and fatigue. So it is necessary to account for the acceleration due to the synergistic interaction of fracture processes in corrosion fatigue crack growth to conservatively predict the life of the structural components of Alloy 600 in corrosive nuclear environments. © 1999 Published by Elsevier Science B.V. All rights reserved.

PACS: 81.40.N

1. Introduction

Corrosion fatigue is a material degradation process in the environment in which fracture processes of fatigue and stress corrosion operate simultaneously. Degradation of structural materials such as those of the nuclear pressure vessel and steam generator tubes occurs by low cycle corrosion fatigue. An experimental measurement of the corrosion fatigue crack growth rate in a low fatigue cycle range is difficult because the measurement requires a long test period and also because of the accompanying pollution of the test environment. So various models were developed for the prediction of the corrosion fatigue crack growth rate.

Many models which combine fatigue and stress corrosion effects have been suggested for use in predicting the corrosion fatigue crack growth rate as a function of fatigue loading frequency. These models can be divided into three categories; (1) superposition models [1], (2) competition models, and (3) models [2–5] for environmentally modified material deformation and fatigue properties. The superposition models and the competition models were developed with the assumption that: (1) an environmental fracture process is independent from the mechanical fatigue fracture process and (2) the mechanical fatigue fracture process in a corrosive environment is identical with the process in an inert environment. Environmental degradation and a pure fatigue fracture process occur simultaneously and indepen-

* Corresponding author. Tel.: +82-42 868 2381; fax: +82-42 868 2212; e-mail: gobul20@nanum.kaeri.re.kr

PII: S0022-3115(99)00114-2

dently on the same fracture surface, and have no interaction with each other according to the superposition models. So the total corrosion fatigue crack growth rate is the linear addition of each contribution attributed to the environmental fracture process and the mechanical fracture process, as in this formula:

$$\left(\frac{da}{dN}\right)_{CF} = \left(\frac{da}{dN}\right)_{int} + \left(\frac{da}{dN}\right)_{SCC} \quad (1)$$

In this equation, $(da/dN)_{CF}$ is the total fatigue crack growth length per fatigue cycle, $(da/dN)_{inert}$ the fatigue crack growth length per fatigue cycle in an inert environment, $(da/dN)_{SCC}$ is the stress corrosion crack growth length per fatigue cycle.

The superposition models have explained the corrosion fatigue crack growth behavior relatively well for some corrosion fatigue systems and have been used for the life prediction of structural materials in nuclear reactors. However, there are many cases in which the superposition models cannot be applied properly [6]. In this study, the assumptions of the superposition models are examined by testing the crack growth behavior of Alloy 600 in a simulated nuclear environment under various load types. In addition, the effects of a synergistic interaction between fatigue and stress corrosion cracking on the total corrosion fatigue crack growth in the environments were discussed in this paper.

2. Experimental method

The corrosion fatigue crack growth tests were conducted with the apparatus shown in Fig. 1. The chemical composition of the Alloy 600 material for the test is shown in Table 1. Compact tension (CT) specimens were used for the crack growth test. Fatigue loads were applied to the CT specimens with a servo hydraulic compression-tension testing machine. Three types of loads, as shown in Fig. 2, were applied. Load type 1 is applied to simulate pure fatigue, load type 2 is to simulate stress corrosion, and load type 3 is to combine the load of fatigue and stress corrosion. High temperature water in the autoclave in Fig. 1 was circulated continuously by a high pressure pump to maintain a constant corrosion environment. Dissolved oxygen concentration was controlled within 4–6 ppm by supplying the mixed O_2 and N_2 gas to the water tank continuously. The crack growth length was measured by a crack opening displacement (COD) gauge which is attached to the specimen.

3. Test Results

3.1. Corrosion fatigue crack growth rate

The fatigue crack growth test was carried out in high temperature water at 290°C. The fatigue load was applied at a frequency of 0.167 Hz and at a load ratio (R) of 0.2. The corrosion fatigue crack growth rate under load type 1 is shown in Fig. 3 as a function of ΔK. The curve for fatigue crack growth rate (da/dN) vs. ΔK shows linearity when ΔK is above 25 MPa $m^{1/2}$. Crack closure seems to influence the crack growth behavior below ΔK of 25 MPa $m^{1/2}$. The crack closure loads in Alloy 600 during a fatigue test in air at room temperature are shown in Fig. 4. Below ΔK of 25 MPa $m^{1/2}$, crack closures appear in Alloy 600 and the magnitude of crack closures increase as ΔK decreases. This fact is reflected in Fig. 3 that the fatigue crack growth rate of Alloy 600 decreases rapidly at ΔK <25 Mpa $m^{1/2}$. A regression line above 25 MPa $m^{1/2}$ of ΔK, shown in Fig. 3, can be represented by this equation:

$$\left(\frac{da}{dN}\right)_{CF} = 10^{-6.68} \times \Delta K^{2.05}. \quad (2)$$

3.2. Stress corrosion crack growth rate

Stress corrosion crack growth rates of Alloy 600, using load type 2, are shown as a function of stress intensity (K) in Fig. 5. The data points of the stress corrosion cracking (SCC) growth rate showed a constant value in the range of stress intensity of this study. The data of SCC growth rates, which were measured in a pressurized water reactor (PWR) environment, are shown in Fig. 5 to compare with the data in this study. A comprehensive curve for the maximum SCC crack growth rate of Alloy 600 includes the data of this study and other data in PWR environments as shown in Fig. 5. The equation of the SCC crack growth curve is represented as

$$\left(\frac{da}{dN}\right)_{SCC} = 5 \times 10^{-11} \times (K-5)^{1.16}. \quad (3)$$

The curve accounts for the test results of this study, other research in PWR environments, and the research [7] in boiling water reactor (BWR) environments. So the SCC crack growth rate of Alloy 600 in various environments can be estimated conservatively by this curve.

3.3. Crack growth rate under composite loads of fatigue and SCC

The crack growth rates under the composite load (type 3) of fatigue and SCC as a function of stress intensity are shown in Fig. 6. The fatigue crack growth length per fatigue cycle under load type 1 at ΔK of 30 MPa $m^{1/2}$ is about 2×10^{-4}mm. In the case of load type 3, the crack growth length per fatigue cycle is about 4×10^{-4}mm at the same value of ΔK. The crack growth rate under load type 3 is faster by a factor of about 2 than that under load type 1. The fatigue crack growth rate under load type 3 can be regressed by

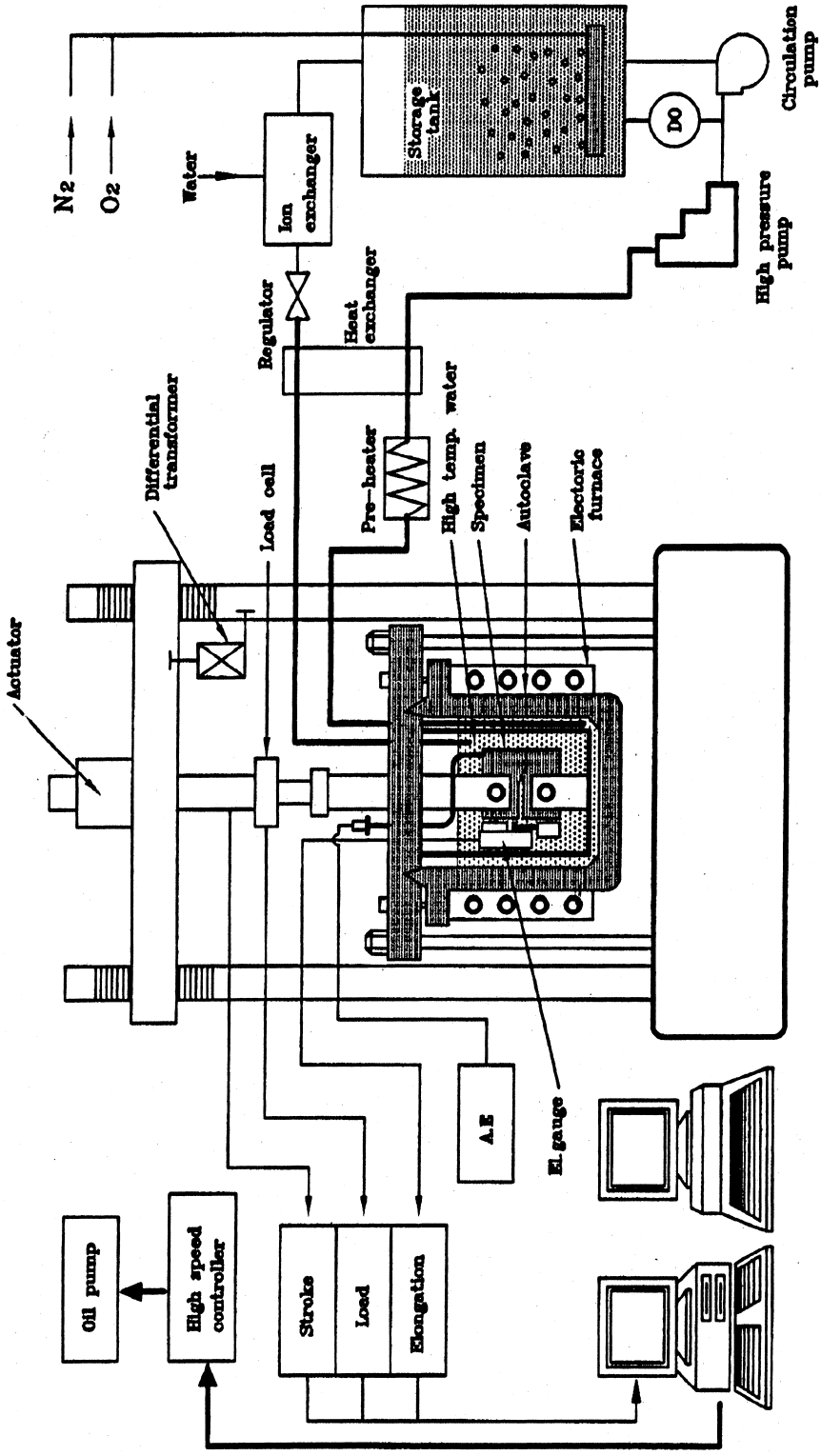

Fig. 1. Diagram of corrosion fatigue testing apparatus (DO: dissolved oxygen sensor, AE: acoustic emission sensor, and EL. gauge: elongation gauge).

Table 1
Composition of Alloy 600 test specimen

Element	C	Mn	P	S	Si	Cr	Ni	Cu	Cb	Ta	Co	Fe
Content (wt%)	0.05	0.20	0.008	0.0003	0.13	15.31	74.897	0.01	0.027	0.011	0.08	8.43

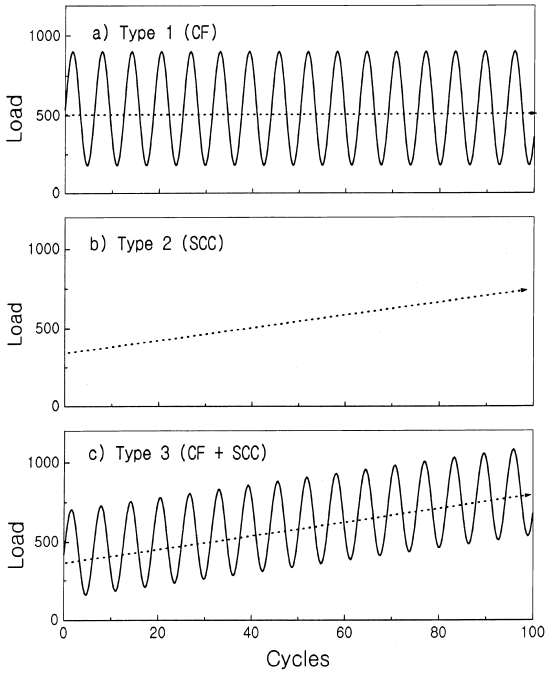

Fig. 2. Types of various applied loads which simulate fatigue, stress corrosion cracking, and mixed mechanism of fatigue and stress corrosion cracking.

$$\left(\frac{da}{dN}\right)_{\text{Type 3 (meas)}} = 10^{-6.15} \times \Delta K^{1.85}. \quad (4)$$

It is confirmed that the fatigue crack growth rate under load type 3 is considerably higher than the growth rate under load type 1.

4. Discussion

It is assumed that there are no interactions among the failure processes that affect the corrosion fatigue crack growth rates according to Wei's superposition model. So the total crack growth rate is the linear addition of the contributions attributed to various crack growth mechanisms. This is expressed by the equation

$$\left(\frac{da}{dN}\right)_{CF} = \left(\frac{da}{dN}\right)_{int} + \left(\frac{da}{dN}\right)_{SCC}.$$

The growth rate, $(da/dN)_{inert}$, can be measured by a fatigue test in inert environments. The stress corrosion

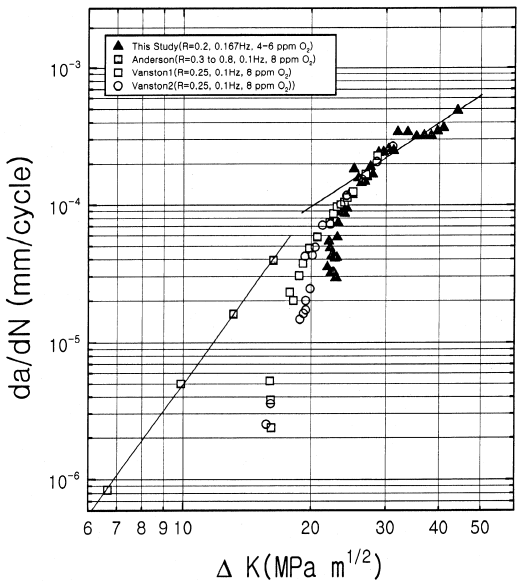

Fig. 3. Corrosion fatigue crack growth velocity of Alloy 600 at 290°C in high temperature water.

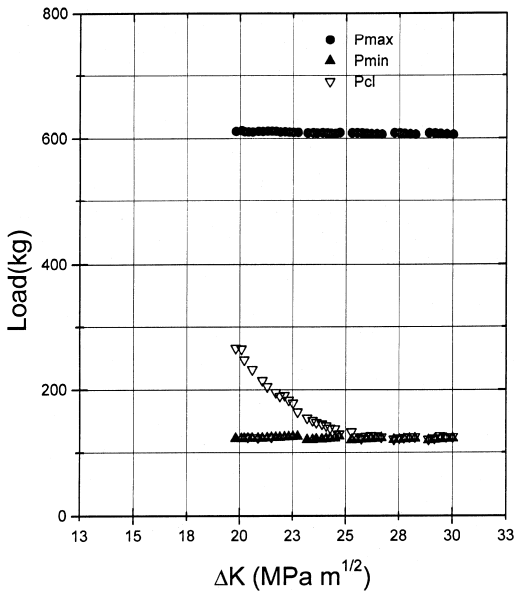

Fig. 4. Crack closure loads during fatigue crack growth test of Alloy 600 at room temperature in air (1 Hz, $R = 0.2$, P_{max}: maximum load, P_{min}: minimum load, P_{cl}: closure load).

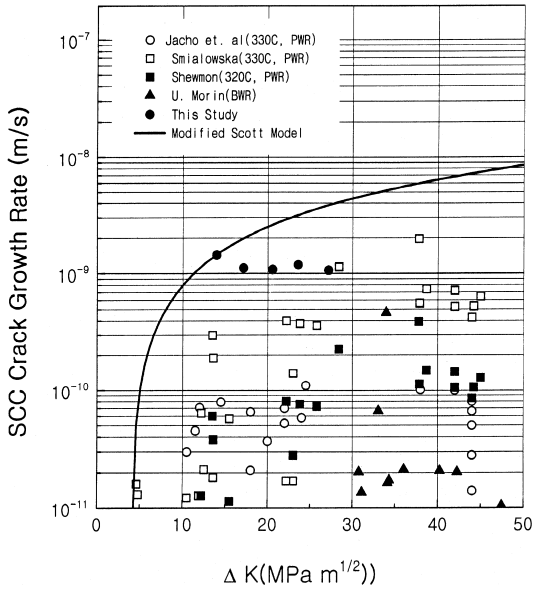

Fig. 5. SCC crack growth rates of Alloy 600 as a function of stress intensity in high temperature water.

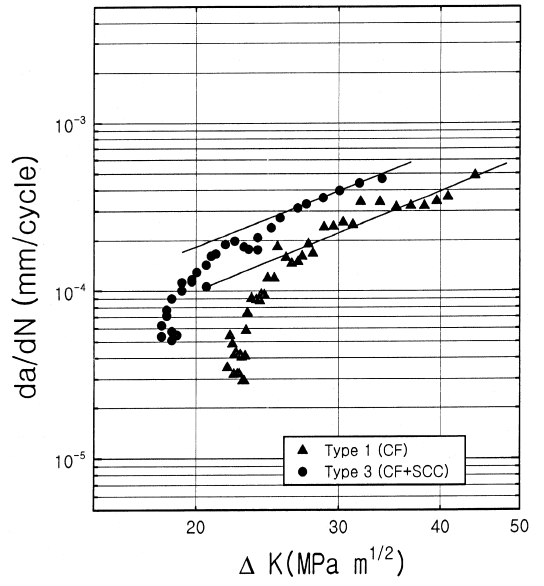

Fig. 6. Corrosion fatigue crack growth rates of Inconel 600 as a function of stress intensity in high temperature water (dissolved oxygen: 4 ppm, applied load: type 1 and type 3).

crack growth rate per fatigue cycle, $(da/dN)_{SCC}$, is usually quantified by mutiplying $(da/dt)_{SCC}$ by load rise time during the fatigue cycle. In this study, load types 1, 2, and 3 were applied separately in crack growth tests to explicitly evaluate the effects of the SCC crack growth rate, $(da/dN)_{SCC}$, on the total corrosion fatigue crack growth rate. The total crack growth rate under load type 3 can be expressed as this equation according to the superposition model

$$\left(\frac{da}{dN}\right)_{\text{Type 3 (Cal)}} = \left(\frac{da}{dN}\right)_{CF} + \left(\frac{da}{dN}\right)_{SCC}. \tag{5}$$

By substituting Eqs. (2) and (3) into Eq. (5), it follows that

$$\left(\frac{da}{dN}\right)_{\text{Type 3 (cal)}} = 10^{-6.68} \times \Delta K^{2.05} + \int_{t_1}^{t_2} (5 \times 10^{-11} \times (K-5)^{1.16})\,dt, \tag{6}$$

where t_1 is the starting time and t_2 is the finishing time of a fatigue cycle during which the fatigue stress intensity range has the value of ΔK. K is the value corresponding to the average load during the fatigue cycle. The value of K can be obtained from the experimental data. The relationship between K and ΔK, which can be established from the experimental data, is represented as

$$K_{\text{mean}} = 1.0133 \times \Delta K - 4.1775. \tag{7}$$

Inserting this equation into the second term of Eq. (6), it follows that

$$\left(\frac{da}{dN}\right)_{SCC} = \int_{t_1}^{t_2} \left(\frac{da}{dt}\right)_{SCC} dt = \int_{t_1}^{t_2} (5 \times 10^{-11} \times (1.0133 \times \Delta K - 9.1775)^{1.16})\,dt. \tag{8}$$

The fatigue cycle time in this test is 6 s. Inserting this time period into Eq. (8), the stress corrosion crack growth rate during fatigue cycle is represented as

$$\left(\frac{da}{dN}\right)_{SCC} = 6 \times 5 \times 10^{-11} \times (1.0133 \times \Delta K - 9.1775)^{1.16}. \tag{9}$$

So, the total crack growth rate according to the superposition model is expressed as follows:

$$\left(\frac{da}{dN}\right)_{\text{Type 3 (cal)}} = 10^{-6.68} \times \Delta K^{2.05} + 3 \times 10^{-10} \times (1.0133 \times \Delta K - 9.1775)^{1.16}. \tag{10}$$

The measured corrosion fatigue crack growth rate under the load type 3 is expressed in

$$\left(\frac{da}{dN}\right)_{\text{Type 3 (meas)}} = 10^{-6.15} \times \Delta K^{1.850}. \tag{11}$$

The crack growth test results under load types 1, 2, and 3 are shown in Fig. 7 along with the calculation result of the total crack growth rate based on the superposition model. In the case of load type 3, the measured crack growth rate is considerably faster than the calculated value based on the superposition model.

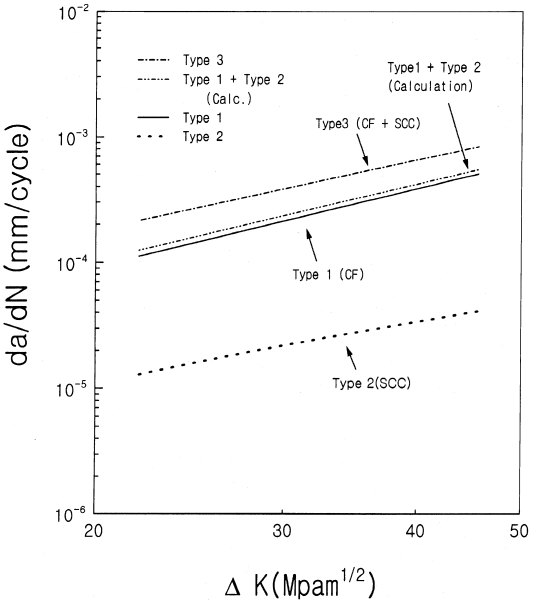

Fig. 7. Comparison of calculated and measured corrosion fatigue crack growth rates of Alloy 600 in high temperature water (dissolved oxygen: 4 ppm, applied load: type 1 and type 3).

The superposition model proposed by Wei et al. was applied successfully to predict the corrosion fatigue crack growth rate of some material-environments systems [8,9]. However, it seems not possible to predict the corrosion fatigue crack growth rate of Alloy 600 in the environment of high temperature water in this study. The total crack growth rate of Alloy 600 in high temperature water is not a linear summation of the mechanical fatigue crack growth rate and the stress corrosion crack growth rate. The difference between the calculated and measured values indicates that the corrosion fatigue cracks under the composite load do not grow by simple superposition of various degradation mechanisms at the crack tip. So it seems that there are synergistic effects on the total crack growth rate due to the interaction of fatigue and stress corrosion mechanism.

Several corrosion fatigue mechanisms were proposed to evaluate the frequency effect on the crack growth rate of various corrosion fatigue systems. Wei et al. [10] suggested that the corrosion fatigue crack growth rate is controlled by the transport and surface reaction rate of material embrittling elements at the crack tip area. They argued the mechanism based on the test results of the crack growth rate of 2219-T851 Al alloy as a function of water vapor pressure. Holroyd and Hardie [6] suggested that the corrosion fatigue crack growth rate was determined by a diffusion mechanism into the material lattice based on the fact that the corrosion fatigue crack growth rates of 7017-T651 Al alloys have a linear relationship with fatigue frequency$^{1/2}$ in a sea water environment. However, there are some corrosion fatigue systems which show the opposite trend. The corrosion fatigue crack growth rates (da/dN) for a rotor steel tested in hydrogen gas [11] and A533B tested in distilled water or 3% NaCl solution [12] decrease as frequency decreases below a critical value. These facts indicate that the fatigue frequency contribution to the SCC crack growth during the corrosion fatigue cycle is not only dependent on load rise time but also on other variables. There seem to be other mechanisms which accelerate SCC crack growth during the corrosion fatigue cycle.

Various investigators [13–18] verified that SCC crack growth is closely related to the fracture of the protective oxide layer by a slip mechanism and the resolution of metal ions at the crack tip area. The mechanism of crack growth by oxidation of the crack tip and resolution of metal ions is called the slip-oxidation mechanism because the mechanism includes the process of metal resolution to metal ion (M/M^+) and the metal oxidation (M/MO). Ford quantified the crack growth rate (V_t) based on the slip-oxidation mechanism with the following equation [19]:

$$V_t = \frac{m}{nDF}\frac{Q_f}{t_{int}}, \tag{12}$$

where m and D are the atomic weight and density of the crack-tip metal, F the Faraday's constant, n the number of electrons involved in the overall oxidation of an atom of metal, t_{int} the time interval of the fracture of the protective oxide layer, and Q_f is the accumulated charge during t_{int}.

4.1. Interaction of fatigue load and SCC

The acceleration of the total crack growth rate in this study can be explained if there is a mechanism of increasing the SCC crack growth rate by alternating fatigue loads. It could be deduced that alternation of fatigue stress can affect the SCC crack growth rate considering the fact that the composite load cycle for SCC and fatigue (load type 3) could accelerate the total crack growth rate considerably without decreasing fatigue frequency. It can be considered that the stress corrosion cracks grow by the slip-oxidation mechanism also during the corrosion fatigue cycle. The fatigue process can influence the SCC crack growth rate like the processes as follows: alternation of fatigue stress could increase the amount of slip at the crack tip. The increase of the number of slips at the crack tip makes the protective oxide layer break with ease, and reduces the time interval, t_{int}. The reduction of time interval, t_{int}, accelerates the SCC crack growth rate according to Eq. (12). There could be some relation between t_{int} and fatigue frequency. If t_{int} is short compared with the fatigue cycle time, there will be little effect on the total crack growth

rate. But if t_{int} is long there will be much influence on the total crack growth rate.

This explanation has some validity considering the fact that the corrosion fatigue systems of stainless steel [8] and 7079-T6 Al alloys [9] which have a high SCC growth rate can be explained relatively well with superposition models. On the other hand, the 7000 series Al alloys [20] which have low SCC growth rates cannot be explained with the superposition models.

The assumption of the superposition model that the mechanical fatigue crack propagation process is the same as the process in the inert environment should be modified to evaluate the crack growth behavior of the wider corrosion fatigue system. It seems that the model of environmentally modified materials deformation and fatigue properties has more validity because the model suggests that the mechanical fatigue fracture and stress corrosion process has an interaction with the environment and accelerates the crack growth rate.

5. Conclusion

When the mechanical fatigue load is applied with the stress corrosion load simultaneously, the two loads could interact and accelerate the crack growth rate. To evaluate the corrosion fatigue crack growth rate and it's interaction with the stress corrosion process in Alloy 600, crack growth tests under three different types of loads which simulate fatigue, stress corrosion, and composite loads of fatigue and stress corrosion, were carried out in 290°C high temperature water with a dissolved oxygen concentration of 4 ppm.

1. The crack growth rate under the fatigue load (the load type 1) in the environment is expressed in the following equation ($R = 0.2$, frequency $= 0.167$ Hz):

$$\left(\frac{da}{dN}\right)_{CF} = 10^{-6.68} \times \Delta K^{2.05}.$$

2. The total corrosion fatigue crack growth rate, when the composite load (load type 3) of pure fatigue and stress corrosion is applied in the environment, is expressed in the following equation (initial $R = 0.2$, frequency $= 0.167$ Hz):

$$\left(\frac{da}{dN}\right)_{\text{Type 3 (meas)}} = 10^{-6.15} \times \Delta K^{1.85}.$$

3. The total crack growth rate of the system is not the linear addition of various fracture processes. The total corrosion fatigue crack growth rate under load type 3 is accelerated by the interaction of the fatigue and the stress corrosion load in the test environment. The synergistic interaction should be accounted for in the conservative prediction of the corrosion fatigue life of Alloy 600 in the environment of a nuclear reactor.

References

[1] R.P. Wei, J.D. Landes, Matls. Res. Stds. ASTM 7 (1969) 25.
[2] S.P. Lynch, Met. Sci. J. 9 (1975) 401.
[3] C.D. Beachem, Metall. Trans. 3 (1972) 437.
[4] S.P. Lynch, Fatigue Mechanisms, ASTM-STP-675, in: J.T. Fong (Ed.), ASTM, Philadelphia, PA, 1979, p. 174.
[5] S.P. Lynch, Hydrogen effects in metals, in: A.W. Thompson, I.M. Bernstein (Eds.), AIME, New York, 1981, p. 863.
[6] N.J.H. Holroyd, D. Hardie, Corros. Sci. 23 (1983) 527.
[7] Ulf Morin, in: Proceeding of the Sixth International Symposium on Environmental Degradation of Materials in Nuclear Power systems–Water Reactors, 1–5 August 1993, San Diego, California.
[8] T. Ishihara, NRIM Rep. 14 (1993) 29.
[9] M.O. Speidel, ICAF Symposium, Lausanne, Switzerland, 1975.
[10] R.P. Wei, P.S. Pao, R.G. Hart, T.W. Weir, G.W. Simmons, Metall. Trans. 11A (1980) 151.
[11] P. Smith, A.T. Stuart, Met. Sci. J. 13 (1979) 429.
[12] J.D. Atkinson, T.C. Lindley, Met. Sci. J. 13 (1979) 444.
[13] T.R. Beck, Corrosion 30 (1974) 408.
[14] H.L. Logan, J. Nat. Bur. Stand. 48 (1952) 99.
[15] R.W. Staehle, in: J.C. Scully (Ed.), Theory of Stress Corrosion Cracking, Brussels, 1971, p. 223.
[16] J.C. Scully, Corros. Sci. 8 (1968) 177.
[17] T.P. Hoar, in: J.C. Scully (Ed.), Theory of Stress Corrosion Cracking, Brussels, Belgium, 1971, p. 106.
[18] D.D. Vermilyea, J. Electrochem. Soc. 119 (1972) 405.
[19] F.P. Ford, Corrosion 52 (1996) 375.
[20] M.O. Speidel, in: M. Arup, R.N. Parkins (Eds.), Stress Corrosion Research, NATO, Sijthoff and Noordhoff, The Netherlands, 1979, p. 117.